Publication Year	2018
Acceptance in OA	2020-11-19T15:17:44Z
Title	Metamaterial-based Toraldo pupils for super-resolution at millimetre wavelengths
Authors	Shitvov, Alexey, Maffei, Bruno, Riminesi, Cristiano, NAVARRINI, Alessandro, ORFEI, ALESSANDRO, Migliozzi, Massimo, D'Agostino, Francesco, OLMI, LUCA, BOLLI, Pietro, Mugnai, Daniela, Tucker, Carole, Pisano, Giampaolo
Publisher's version (DOI)	10.1117/12.2314086
Handle	http://hdl.handle.net/20.500.12386/28454
Serie	PROCEEDINGS OF SPIE
Volume	10708

PROCEEDINGS OF SPIE

SPIEDigitalLibrary.org/conference-proceedings-of-spie

Metamaterial-based Toraldo pupils for super-resolution at millimetre wavelengths

Pisano, Giampaolo, Shitvov, Alexey, Tucker, Carole, Mugnai, Daniela , Bolli, Pietro, et al.

Giampaolo Pisano, Alexey Shitvov, Carole Tucker, Daniela Mugnai, Pietro Bolli, Luca Olmi, Francesco D'Agostino, Massimo Migliozzi, Alessandro Orfei, Alessandro Navarrini, Cristiano Riminesi, Bruno Maffei, "Metamaterial-based Toraldo pupils for super-resolution at millimetre wavelengths," Proc. SPIE 10708, Millimeter, Submillimeter, and Far-Infrared Detectors and Instrumentation for Astronomy IX, 107080G (9 July 2018); doi: 10.1117/12.2314086

SPIE.

Event: SPIE Astronomical Telescopes + Instrumentation, 2018, Austin, Texas, United States

Downloaded From: https://www.spiedigitallibrary.org/conference-proceedings-of-spie on 19 Nov 2020 Terms of Use: https://www.spiedigitallibrary.org/terms-of-use

Metamaterial-based Toraldo pupils for super-resolution at millimetre wavelengths

Giampaolo Pisano*[a], Alexey Shitvov[a], Carole Tucker[a], Daniela Mugnai[b], Pietro Bolli[c], Luca Olmi[c], Francesco D'Agostino[d], Massimo Migliozzi[d], Alessandro Orfei[e], Alessandro Navarrini[f], Cristiano Riminesi[g], Bruno Maffei[h]

[a]School of Physics and Astronomy, Cardiff University, Queen's Building, The Parade, CF24 3AA Cardiff (United Kingdom); [b]IFAC-CNR, Firenze (Italy); [c]INAF-OAA, Firenze (Italy); [d]DIIN, Università di Salerno (Italy); [e]INAF-IRA, Medicina (Italy); [f]INAF-OAC, Cagliari (Italy); [g]ICVBC-CNR, Firenze (Italy); [h]IAS, Orsay (France)

ABSTRACT

Using the long-established Cardiff metal-mesh filter technology, we have exploited our ability to artificially manipulate the phase of a wavefront across a device in order to produce a dielectric-based Toraldo pupil working at millimeter wavelengths. The use of a Toraldo pupil to push the angular resolution of an optical imaging system beyond the classical diffraction limit is yet to be realized in the millimeter regime, but is an exciting prospect. Here we present the design and measured performance of a prototype Toraldo pupil, based on a 5 annuli design.

Keywords: Radioastronomy, Optics, millimeter-wave instrumentation, super resolution.

INTRODUCTION

In 1952, G. Toraldo di Francia proved that in principle the angular resolution of an optical imaging system can go beyond the classical diffraction limit [1]. The concept of super-resolution was discussed by studying the diffraction from a circular aperture as the sum of a finite number of emitting coronae, with different amplitudes and phases. By choosing particular combinations of these coefficients, i.e. by manipulating the radiation across these coronae within the aperture, it is theoretically possible to achieve any desired resolution. However, the angular resolution improvement comes at the expenses of increased radiation diffracted at large angles, i.e. an increase of the side-lobes. Between the main lobe and the side-lobes there is a dark angular corona which can be extended by increasing the number of coronae.

In 2003, the above concept was verified by realizing and successfully testing a 'Toraldo Pupil' working at microwave frequencies. Later realizations have confirmed the principle and have proven that Toraldo Pupils could be implemented within the optical systems of radiotelescopes in order to improve their angular resolution.

The Toraldo Pupils realized so far are made of concentric dielectric rings interspaced with circular air gaps. The dielectric rings are designed to add a 180 degree phase-delay compared to the radiation passing through the air gaps. Although these devices are easy to manufacture, they are designed to work at specific frequencies, they suffer diffraction and mismatch effects from the ring edges and from their holding structures.

In this work we present an alternative approach for the design of Toraldo Pupils based on the metal-mesh filter technology. This technology, successfully used in many millimeter and sub-millimeter astronomical instruments, has been pushed further by developing flat mesh-lenses, mesh half-wave plates, and other more exotic devices. The proven ability to arbitrarily manipulate the amplitude and the phase across a metamaterial surface allows us to design devices able to add the specific phase-delays, which are required by the Toraldo Pupils. Here we present the design and the preliminary test results of a flat, mesh-based Toraldo Pupil working at millimeter wavelengths.

*giampaolo.pisano@astro.cf.ac.uk; phone +44(0)29208 75314.

Millimeter, Submillimeter, and Far-Infrared Detectors and Instrumentation for Astronomy IX,
edited by Jonas Zmuidzinas, Jian-Rong Gao, Proc. of SPIE Vol. 10708, 107080G
© 2018 SPIE · CCC code: 0277-786X/18/$18 · doi: 10.1117/12.2314086

Downloaded From: https://www.spiedigitallibrary.org/conference-proceedings-of-spie on 19 Nov 2020
Terms of Use: https://www.spiedigitallibrary.org/terms-of-use

TORALDO PUPILS

Toraldo's analytical model

Toraldo's model can be summarized as follow. Let us consider a circular corona illuminated by a plane wave. The diffracted amplitude A in the θ direction is given by (far field):

$$A(\theta) = \frac{A_0}{2\lambda \sin\theta} \left[d_2 J_1\left(\pi \frac{d_2}{\lambda} \sin\theta\right) - d_1 J_1\left(\pi \frac{d_1}{\lambda} \sin\theta\right)\right],$$

where d_1 and d_2 are the internal and external diameters, respectively, A_0 is the uniform complex-amplitude that illuminates the corona, λ is the wavelength and J_1 is the Bessel function of the first order. Let us now consider a pupil of diameter d, and let us assume that the pupil is divided into n circular coronae, the diameter of which can be denoted by $a_0 d, a_1 d, a_2 d \cdots a_n d$, where $a_0 \cdots a_n$ are a succession of numbers in increasing order, with $a_0 = 0$ and $a_n = 1$. By exchanging the angular coordinate with a linear one, namely by using $(\pi d/\lambda) \sin\theta$, the total amplitude diffracted by the composed pupil can be written as

$$A(x) = \sum_{i=0}^{n-1} \frac{\gamma_{i+1}}{x} \left[a_{i+1} J_1(\alpha_{i+1} x) - a_i J_1(\alpha_i x)\right], \tag{1}$$

where the quantity $\gamma_{i+1} = (\pi d^2/2\lambda^2)\, I_{i+1}$ is a constant proportional to the amplitude I_{i+1} that illuminates each corona. Looking at Eq. (1), we can see that by imposing the values of the zeros of the diffracted amplitude, we have a system of n equations from which we can evaluate the coefficient $\gamma_1 \cdots \gamma_n$, namely the amplitude that the incident wave must have, in order to obtain exactly the diffracted amplitude that we want. In other words, we can establish the width of the main lobe and obtain the super-resolution effect. The general solution of Eq. (1) describes a system in which each corona is transparent and characterized by a different amplitude, depending on the geometric characteristics of the composed pupil. But, more important, there is a phase inversion between one corona and the other, and this condition alone is sufficient to produce super-resolution.

Laboratory measurements in the microwave range

The first measurements in the microwave range ($\simeq$ 10 GHz) were performed in 2003 [2]. The experimental setup used a three-coronae Toraldo Pupil (or TP3), as shown in Fig. 1. The near-field measurements experimentally confirmed the Toraldo prediction about the super-resolution (see Fig. 2). The same measurements were repeated in 2004 in the far-field [3], and again showed the super-resolution effect.

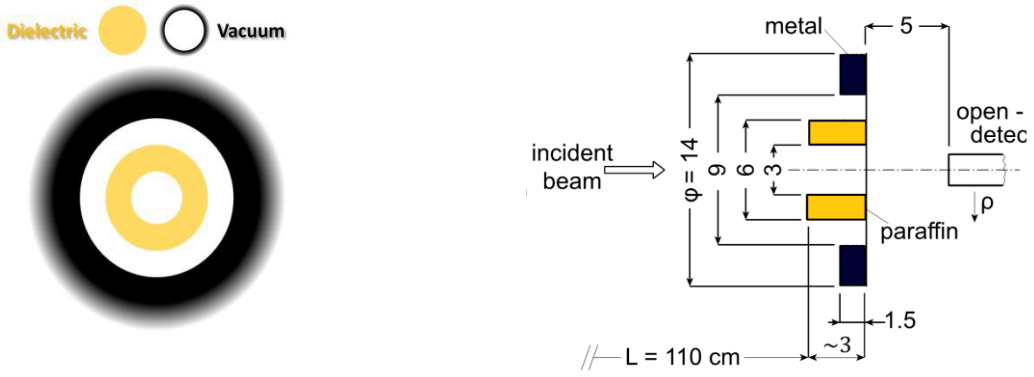

(a) (b)

Figure 1. a) Schematic representation of a TP3. The corona introducing the 180° phase delay (in yellow) is here composed by a dielectric material with the appropriate optical thickness. Sketch of a classic dielectric ring based Toraldo Pupil. b) TP3 used by Mugnai et al. 2003[2]. The central corona consisted of a paraffin torus placed in the middle of a metallic frame and produced a phase delay of 180°, as required (all dimensions are in cm). The near-field was sampled by an open-end waveguide, connected to the detector, which could be moved along the coordinate ρ.

Downloaded From: https://www.spiedigitallibrary.org/conference-proceedings-of-spie on 19 Nov 2020
Terms of Use: https://www.spiedigitallibrary.org/terms-of-use

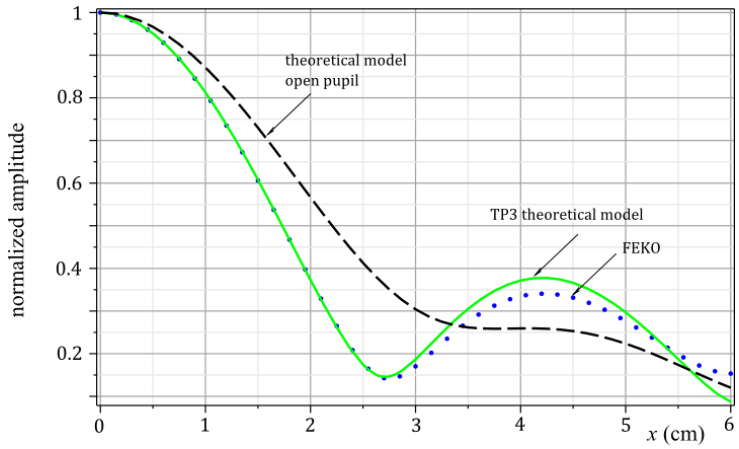

Figure 2. Normalized amplitude (at 20 GHz) for the TP3 (see Fig. 1a) evaluated in the near-field by the analytical model (solid green line) and by an EM simulation using the commercial software tool FEKO [4] (dotted blue line). Both curves can be compared with the amplitude of the corresponding open pupil (dashed black line). The diameters of the coronae are the same as in Fig. 1b, and the distance between the TP and the screen was 18 cm.

The original analytical description of the TP given by Toraldo assumed an ideal optical system where, for example, the phase masks are infinitely thin and an ideal source is assumed that achieves both the required amplitude apodization and uniform phase illumination over the pupil. In the context of the "*Pupille Toraldo*" (PUTO) project [5], and in order to compare the performance of the dielectric-based TP with Toraldo's ideal model we carried out systematic EM simulations of the performance of simple 3D dielectric-based TPs [6], followed by laboratory measurements [7], which extended and improved the initial tests in the microwave range [2, 3], as described above.

If we define the super-resolution gain as G_{SR} = FWHM[open pupil]/FWHM[TP], where FWHM represents the width of the central lobe of the point spread function (PSF), then during these early tests we achieved gains 1.5-1.7, and sidelobes level <~ -5 dB. We also found that, despite being intrinsically monochromatic, the super-resolution effect showed a negligible degradation over a ~ 400 MHz at 20 GHz. However, the efficiency needs to be improved, since the presence of a dielectric-based TP can attenuate the signal by several dBs (also because of back-scattered radiation).

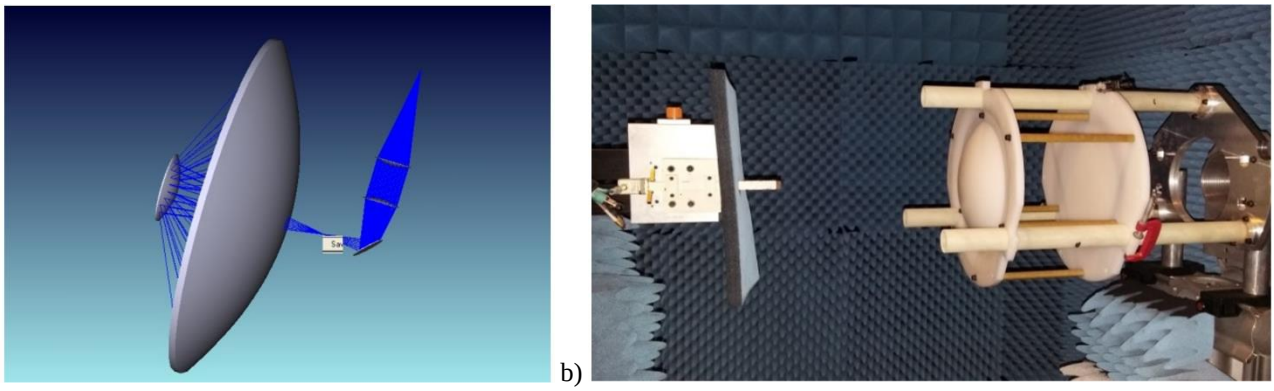

Figure 3. a) Schematic representation of a Cassegrain telescope with a two-lens collimator placed behind the Cassegrain focus. The phase mask (in red) is placed between the two lenses. b) The two-lens collimator under test in the anechoic chamber of the Arcetri Astrophysical Observatory. On the right a corrugated feed-horn simulates the Cassegrain focus, while the near-field after the collimator is sampled by a waveguide probe.

Design and fabrication of a prototype TP optical module for the Medicina radiotelescope

The next step of this project consisted in the design, fabrication and test of a prototype TP optical system to be mounted on a radio telescope [8]. Our preliminary design is based on a two-lens collimator placed after the Cassegrain focus (see Fig.3; a two-mirror collimator could also be used). The first lens of the collimator generates an image of the primary at a position where a phase mask can be applied. The modified wavefront is then brought to a relayed focus by the second lens.

Downloaded From: https://www.spiedigitallibrary.org/conference-proceedings-of-spie on 19 Nov 2020
Terms of Use: https://www.spiedigitallibrary.org/terms-of-use

Because the TP optical module was supposed to be field-tested on the 32-m Medicina radiotelescope, its design had to take into account several opto-mechanical constraints to allow the collimator to be retrofitted on the 18-26.5 GHz dual-horn receiver currently operating on the Medicina antenna [9].

Extensive laboratory measurements were performed on the collimator to characterize the optical system in preparation for the field-tests at the antenna, and confirmed that the super-resolution effect could be achieved with this optical configuration [9, 10]. However, our measurements also showed that when the waveguide probe (which was used to sample point-by-point the electric field in the focal plane of the collimator, see Fig.3) is replaced by a corrugated feed-horn, identical to that mounted on the Medicina K-band receiver, the super-resolution effect is completely wiped out. We think that this effect is caused by a strong mismatch between the fields generated by the collimator and those at the aperture of the feed-horn. The subsequent field-tests at Medicina (see Fig.4) confirmed this result, but they also showed that the basic collimator optical layout was correctly operating [9, 10].

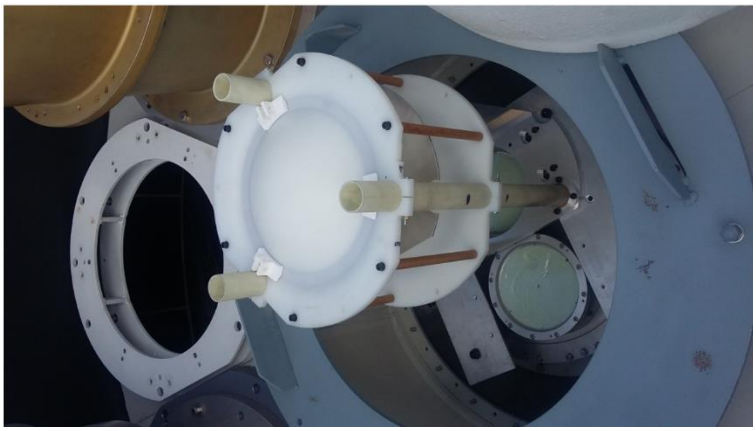

Figure 4. The two-lens collimator installed on the K-band receiver at Medicina and ready for the field-tests.

METAMATERIAL BASED TORALDO PUPILS

The EM simulations and experimental results summarized above show that TPs for the microwave range are very easy to fabricate using 3D dielectric coronae. However, this simple design does not allow to achieve an optimum trade-off between super-resolution-gain, efficiency, sidelobes and bandwidth. Therefore, a different approach must be used to implement an efficient super-resolving optical module based on TPs suitable for radioastronomical applications at both cm- and mm-wavelengths.

In this work we discuss for the first time how metamaterials can be employed to design new types of Toraldo pupils. Here we refer to a particular subset of metamaterials, those related to the mesh-filters technology. This technology has been employed for decades in millimeter and sub-millimeter astronomy instrumentation to allow for thermal shielding and to define the spectral sensitivity of the detectors [11, 12]. More recently the same technology has been advanced further and new devices have been developed, such as mesh-lenses [13], mesh-HWPs [14] and AMC-based reflective HWPs [15, 16]. In relation to these recent developments, we hereafter describe three ways to design TPs using the mesh technology.

Downloaded From: https://www.spiedigitallibrary.org/conference-proceedings-of-spie on 19 Nov 2020
Terms of Use: https://www.spiedigitallibrary.org/terms-of-use

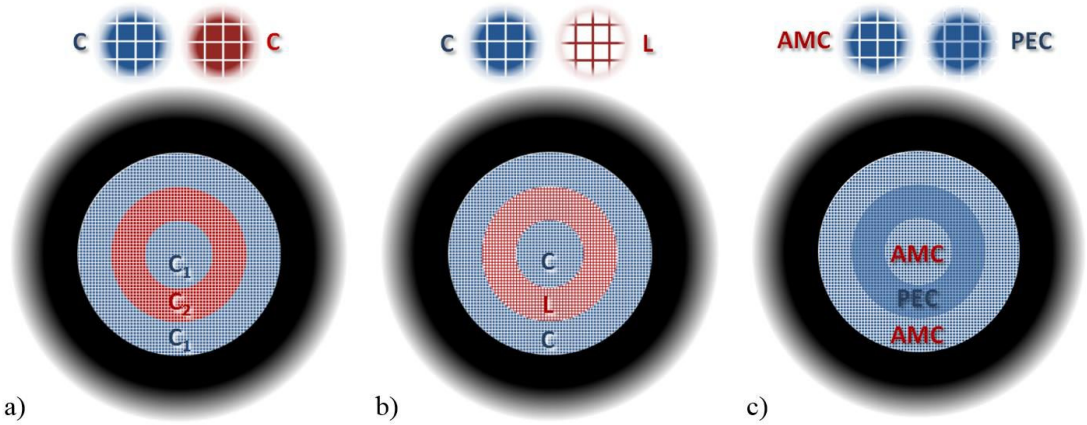

Figure 5. Metamaterial based Toraldo pupil designs: a) Capacitive grids TP; b) Capacitive and inductive grid TP; c) Artificial Magnetic Conductor based TP (working in reflection).

Capacitive grid based TP

Low-pass mesh filters are made of stacked capacitive grids. Each grid comprises an array of subwavelength square patches on a polypropylene substrate (see top Fig. 5a). The grids are kept separated at specific distances by means of other polypropylene substrates and eventually the whole stack is hot-pressed together to form a solid multi-layered metamaterial slab. Capacitive low-pass filters can be designed to cut off high frequencies from tens of GHz to tens of THz. While the in-band transmission can be kept as high as 99%, the large parameter space allows also to achieve specific transmitted phase-shifts, normally ignored in filter design. This property has been used recently to design highly transmissive inhomogeneous surfaces able to arbitrarily vary the phase-shift across them. By tailoring the phase behavior with the position it was possible to design flat mesh-lenses [13].

The mesh-lens structure is composed of subwavelength pixels providing a local phase-shift increasing radially from the central reference pixel. Depending on the lens focusing power the local phase-shifts can easily exceed 180°. A mesh-based Toraldo pupil will be a device made of just two types of capacitive filters (C_1 and C_2) that would provide very high transmission (~99%) and a differential phase-shift equal to 180°. Each type of filter will populate the different coronae of the pupil as sketched in Fig. 5a. The bandwidth of the device will depend also on the differential phase-shift of the pixels as a function of frequency. The only drawback of this design is the number of grids required which can be of the order of twenty.

Capacitive and inductive grid based TP

A slightly different approach to design mesh-based TPs consists in using capacitive and inductive grids for the alternating coronae (C and L), as shown in Fig. 5b. Capacitive and inductive filters provide phase-shifts with opposite signs. A mesh-TP can be designed using homogeneous capacitive and inductive grids where the required 180° phase-shift can be achieved with a relatively small number of grids, i.e., five or six. This property has been used in the past to develop wideband artificial birefringent materials and mesh-HWPs [14], based on anisotropic grids.

Artificial Magnetic Conductor (AMC) based TP

A mesh-based TP can be designed to work in reflection. The 180° differential phase-shifts can be obtained by reflecting the radiation off annular rings made with perfect electric conductor (PEC) and artificial magnetic conductor (AMC) surfaces, as shown in Fig. 5c. An AMC surface has the property to provide an almost null phase-shift in reflection, while a normal PEC surface provides 180°. The AMC developed using the mesh technology has been employed to realize magnetic mirrors [16] and ultra-wideband reflective HWPs [15]. In this work we have explored this third option and realized a 5-coronae AMC-based TP working around 100 GHz.

Downloaded From: https://www.spiedigitallibrary.org/conference-proceedings-of-spie on 19 Nov 2020
Terms of Use: https://www.spiedigitallibrary.org/terms-of-use

AMC-BASED TORALDO PUPIL

Working principle

While a metallic surface provides a 180° phase-shift in reflection, null phase-shifts in reflection can be achieved at interface between high and low permittivity materials when the electromagnetic wave is incident from the high-permittivity medium. A device made with two slabs, the first with high and the second with low permittivities, followed by a backshort, will behave like an AMC surface (see Fig. 6a) providing an almost null phase-shift across a large bandwidth. See references [15, 16] for more details.

By embedding a metal surface within the high-to-low permittivity interface, the phase-shift will be reverted to 180°. If the metal surface has the pattern shown in Fig. 6b, where the black is metal, the device will provide null phase-shift reflection from the apertures (AMC) and 180° everywhere else (PEC). Given the proper dimensions of the apertures, this device may satisfy the condition of a 5-coronae Toraldo pupil working in reflection. The rings are elliptical to compensate for the 45° incidence projection. The Toraldo pupil dimensions are 15×21.2 mm.

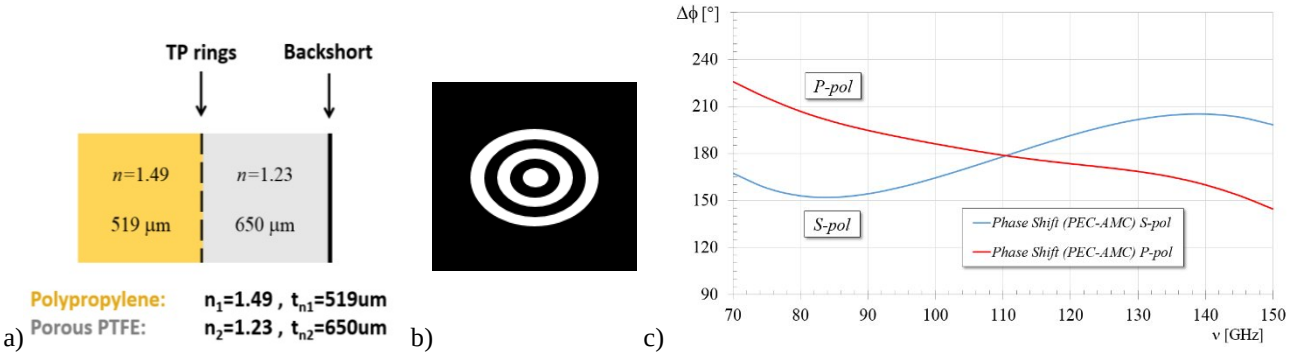

Figure 6. a) Sketch of the embedded AMC-based TP. b) Drawing of the mask used during the photolithographic processes to produce the copper pattern located at the high-to-low index interface of the magnetic mirror. c) Simulated differential-phase shift between PEC and AMC parts of the Toraldo pupil for the two linear polarizations S and P.

Finite element modelling and design

The AMC/PEC surface was modelled using finite-element analysis (Ansys HFSS [17]), assuming an operating frequency of 110 GHz and 45° angle of incidence, for both the S and P polarizations. The first and second slabs were respectively made of polypropylene (n~1.49) and porous PTFE (n~1.23). The metal pattern, as well as the backshort, were simulated as infinitely thin PEC sheets. The slab thicknesses were optimized following the procedure described in [16]. The optimized differential phase-shifts between the PEC and AMC parts of the TP device are plotted as a function of frequency in Fig. 6c for both the S and P polarizations.

The whole Toraldo pupil was modelled using HFSS. Gaussian beams with both S and P polarizations were set at 45° incidence and their beam waists were located at the TP center (see Fig. 7). Radiation boundaries and symmetry planes were assigned to the model. Fig.8 shows the simulation of a Gaussian beam reflecting off a PEC mirror at 45° and the effect of the 5-coronae embedded TP onto the same beam. The corresponding beam cuts are shown in Fig.9. The reference 100 GHz Gaussian beam (beam waist of 9 mm) with ~7° full width at half maximum (FWHM) is reduced down to a narrower beam with ~5.1° FWHM, i.e., a reduction down to ~73% of the original value (a gain G_{SR} ~1.4). This is achieved at the expense of higher sidelobes, in this case reaching -12 dB.

Downloaded From: https://www.spiedigitallibrary.org/conference-proceedings-of-spie on 19 Nov 2020
Terms of Use: https://www.spiedigitallibrary.org/terms-of-use

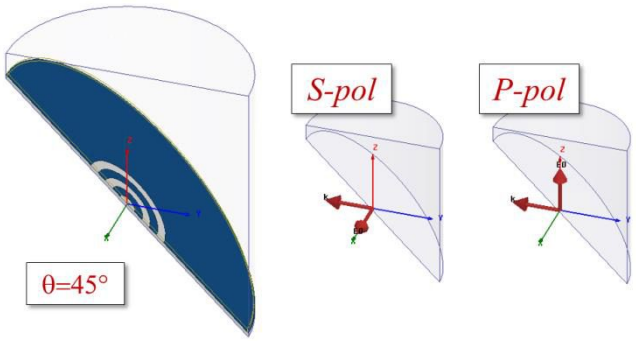

Figure 7. HFSS model of the AMC-based TP with the polarization vector definitions.

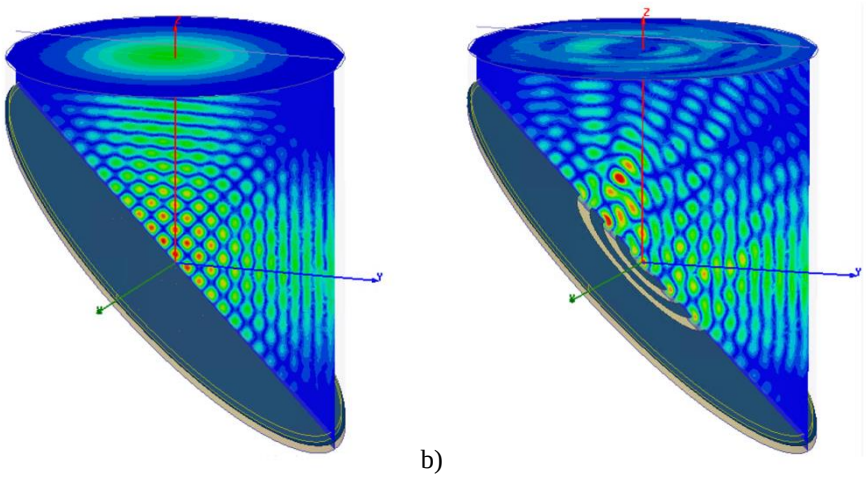

a) b)

Figure 8. a) Finite-element simulation of a Gaussian beam reflected by a PEC mirror; b) Simulation of the interaction of a 5-coronae embedded TP with the reference Gaussian beam. The beam waist is located in the *xz*-plane at the center of the TP.

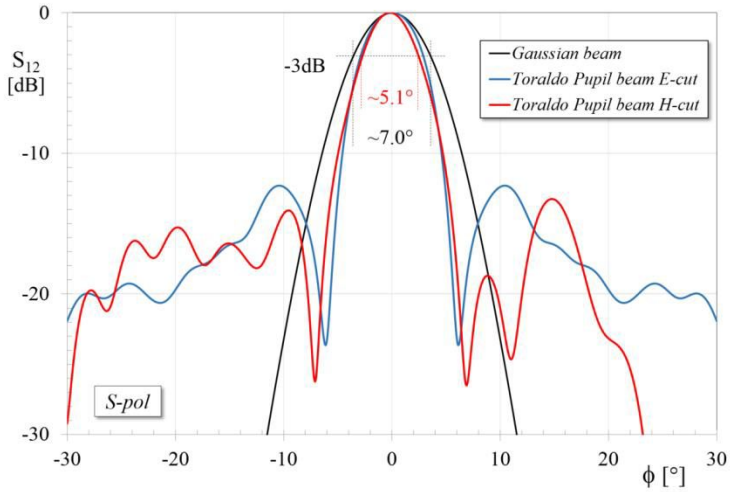

Figure 9. Beam transformation induced by the 5-coronae embedded TP on a Gaussian beam with beam waist 9 mm centered with the pupil.

Downloaded From: https://www.spiedigitallibrary.org/conference-proceedings-of-spie on 19 Nov 2020
Terms of Use: https://www.spiedigitallibrary.org/terms-of-use

TORALDO PUPIL MANUFACTURE

The multi-layer Toraldo plate assembly was manufactured using standard Cardiff University mesh-technology manufacture techniques [11]. The Toraldo pupil pattern was produced by photo-lithographically patterning a 400 nm evaporated Cu film supported on a 10 μm polypropylene substrate. In accordance with Figure 3a the TP was sandwiched between pPTFE and PP slabs and a solid Cu backshort added. This assembly was fused together using the Cardiff hot-pressing techniques, with LDPE used as a gluing layer. The final device and the details of its rings are respectively shown in Fig. 10a and Fig.10b.

a) b)

Figure 10. a) The embedded Toraldo pupil prototype operating in the W-band; b) Close-up view of the embedded TP sample.

EXPERIMENTAL CHARACTERIZATION

Experimental setup

The W-band prototype of the 5-coronae embedded Toraldo Pupil with nested concentric elliptical rings has been measured in the far field using an automated beam-scanning testbed, see Fig. 11. A W-band single-mode corrugated Winston horn antenna [18] was used as a Gaussian beam source emitting a linearly polarized electromagnetic wave with low sidelobes and cross-polarization. The sample was positioned vertically, with the TP at 50 mm distance from the horn aperture, and tilted by 45° to the incident wave axis. The orientation of the VNA head was such that the TP was tested using S-polarization. The major axes of the embedded elliptical coronae were oriented horizontally, so that the aperture appeared visually as circular when viewed from the transmitter direction.

In our experiment, the sample was positioned in the diverging field of the horn antenna whereas in practical radiotelescope applications the TP will be located at the beam waist of a Gaussian beam telescope, either made with lenses or mirrors. In the present study we wanted to reproduce the effects uniquely generated by the TP without additional systematics induced by the Gaussian beam telescope components. The main goal of the experiment was to demonstrate close agreement with simulations, bearing in mind that the demonstrated performance is not optimal.

The transmitter VNA head and the TP sample were mounted on a horizontal arm bolted to a precision rotary stage, so that both could rotate as a whole about the axis corresponding to the virtual waist of the beam, i.e. 50 mm behind the TP sample (see Fig. 11). The receiver head was fixed and had a circular waveguide probe, instead of a standard horn, to reduce standing waves with the TP system. By rotating the above system the receiver could azimuthally scan the phase front of the diverging Gaussian beam reflected off the TP sample. The probe was set at 580 mm from the sample center, measured when the transmitter and receiver were at 90°, i.e. when the scan angle was $\phi = 0°$.

The precision rotary stage motor was driven by a motion controller Newport MM4006. The VNA and motion controller were integrated into a measurement system with the aid of the LabView software and National Instruments GPIB interface cards, see Fig. 11(c). The data acquisition and postprocessing were automated using the standard LabView environment aided with Python scripts.

Downloaded From: https://www.spiedigitallibrary.org/conference-proceedings-of-spie on 19 Nov 2020
Terms of Use: https://www.spiedigitallibrary.org/terms-of-use

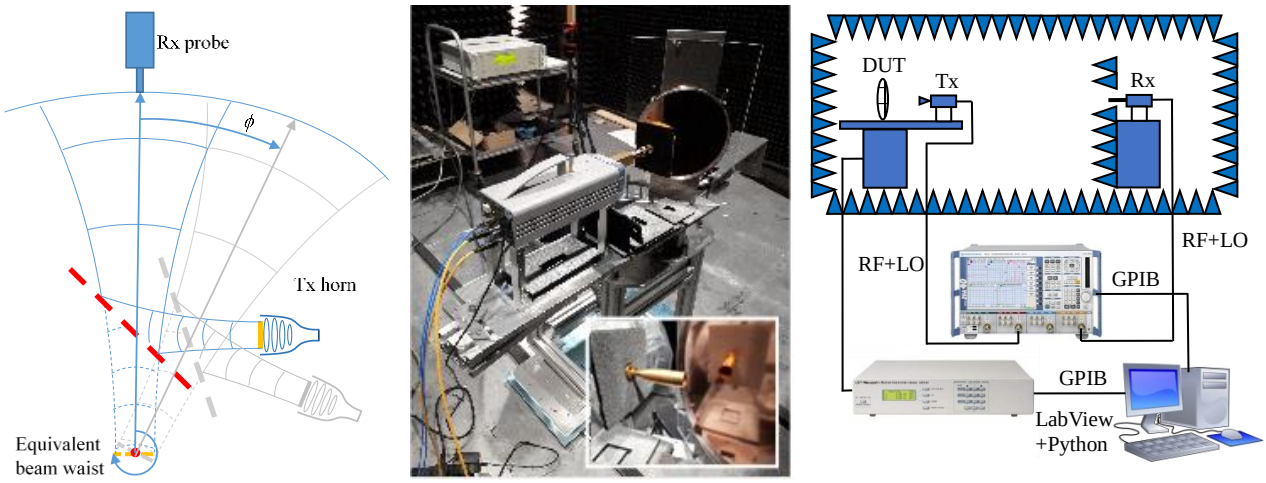

a) b) c)

Figure 11. a) Optical sketch of the beam-measurement testbed, (b) photograph of the experimental setup showing the Tx horn launching the S-polarized wave upon the TP sample (shown in the inset), both mounted on the rotating arm, and (c) the schematic of the automated measurement system controlled by the LabView software.

Beam scans

The S21 measurements were taken in the W-band frequency range (75-110 GHz) using a commercial Rohde & Schwarz ZVA-67 analyzer equipped with ZVA-Z110 frequency converters. At each angular position of the device under test (DUT) measurements were taken twice, in each forward and reverse rotation directions, in order to minimize the RF noise and compensate rotational backlash, thus ensuring better quality of the data. The experiment was conducted in an anechoic chamber where radiation absorbing material (Eccosorb) was used to reduce the standing wave effects.

The first scan was carried out with a copper mirror located in place of the Toraldo pupil. The measured and simulated reflection magnitude versus scanning angle are shown in Fig. 12a. This data represent the reference beam of the corrugated horn reflected off the mirror at 45°. The HFSS model was modified to be more realistic by inserting the geometry of the corrugated horn within the finite-element model. This allowed generation of the real Gaussian beam together with the inherent sidelobes of the source antenna (see Fig. 12b).

The model and the data are in good agreement about the main beam, i.e., within a ±15° range, whereas some discrepancy is observed towards the side lobes. This is due to the size of the model which was limited by the computational resources of the PC running these simulations. However, we are interested in quantifying the effects of the TP on the main beam and the data comparison between measurement and simulation will be limited to the above range. The measured and simulated FWHM of the beam is about 14°, which also in a good agreement with the results presented in [18].

The measured and simulated results for the embedded TP with elliptical coronae are shown in Fig. 13(a), alongside the fields generated by the finite-element simulations (Fig. 13(b)). The device demonstrated a FWHM < 6° and sidelobe level between -3 and -5 dB. The simulated results are in good agreement with the measurement. The observed discrepancy can be attributed to inaccuracies in the sample and antenna alignment.

Downloaded From: https://www.spiedigitallibrary.org/conference-proceedings-of-spie on 19 Nov 2020
Terms of Use: https://www.spiedigitallibrary.org/terms-of-use

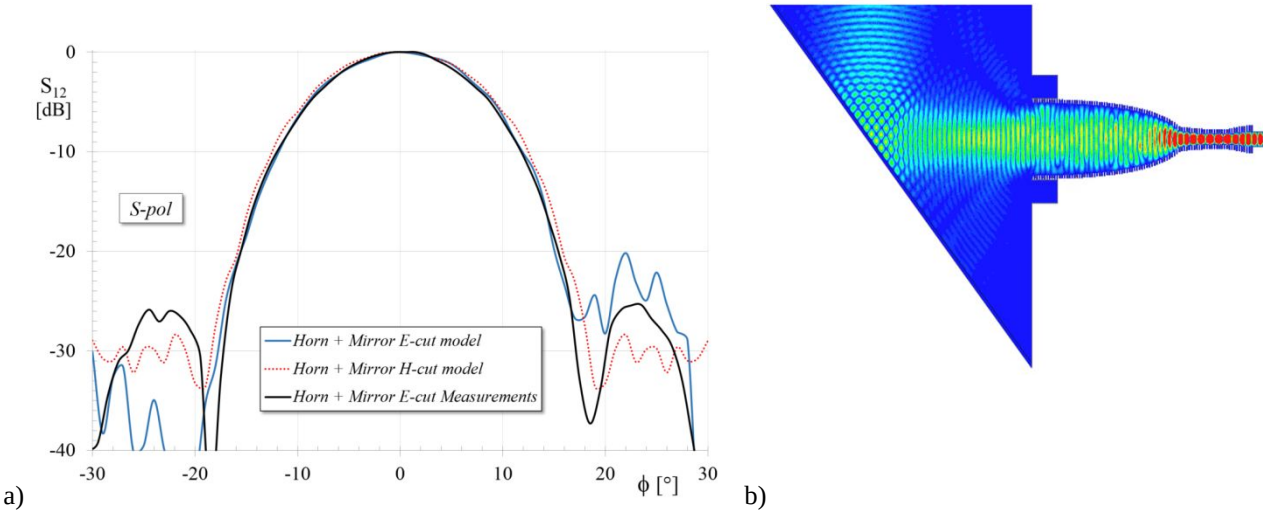

Figure 12. a) Modelled and measured reflection magnitude versus azimuthal angle of the corrugated horn beam reflected off the PEC/copper mirror; b) Fields generated by the finite-element simulations including the corrugated horn geometry. All results are shown at 100 GHz frequency.

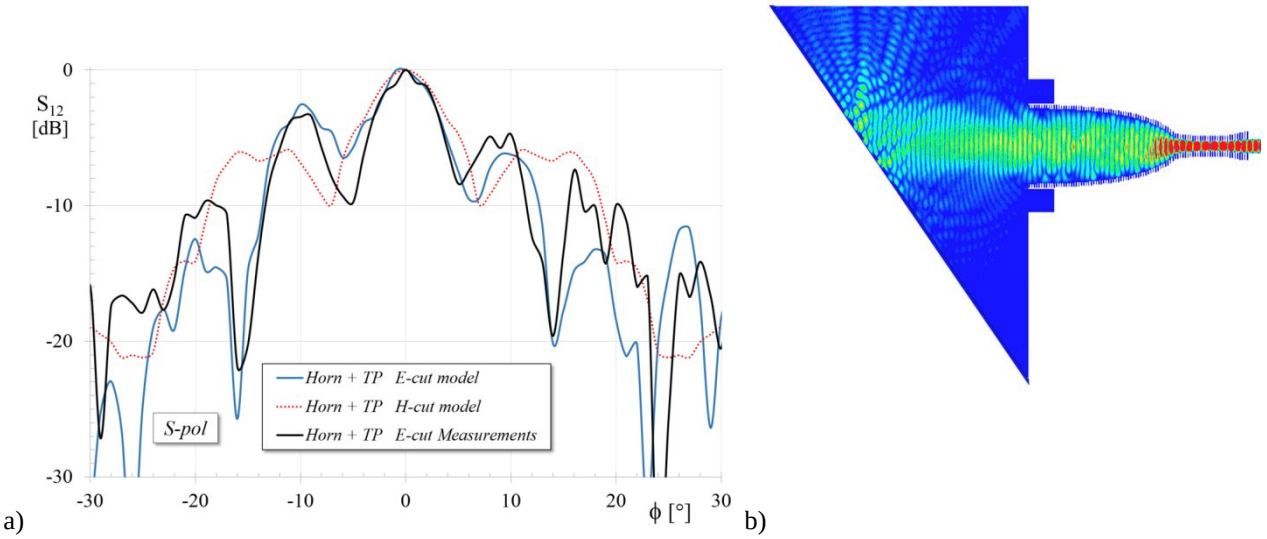

Figure 13. a) Measured reflection magnitude versus azimuthal angle of the embedded TP; b) Fields generated by the finite-element simulations. All results are shown at 100 GHz frequency.

CONCLUSIONS

We have proposed for the first time to use metamaterials to design Toraldo pupils. Three different approaches based on the mesh technology were presented. A 5-coronae embedded Toraldo pupil based on AMC/PEC surfaces was designed, manufactured and successfully tested. The TP was characterized at 100 GHz using the divergent beam of a corrugated horn. The results were in close agreement with the finite-element predictions. The same models shows that the embedded Toraldo pupil, when located in the beam waist of an ideal Gaussian beam telescope, is able to narrow a beam down to ~73% of the original FWHM, while keeping the sidelobe levels below -12 dB. Further work will be dedicated to the characterization of the TP in a Gaussian beam telescope setup, which will be the one used in the real radiotelescope application.

Downloaded From: https://www.spiedigitallibrary.org/conference-proceedings-of-spie on 19 Nov 2020
Terms of Use: https://www.spiedigitallibrary.org/terms-of-use

ACKNOWLEDGMENTS

This work was supported by the STFC Consolidated Grant ST/N000706/1 awarded at Cardiff University and the 'Fondazione Cassa di Risparmio' of Florence.

REFERENCES

[1] G. Toraldo di Francia, "Super-gain antennas and optical resolving power", Il Nuovo Cimento (suppl.), v. IX, n. 3, pp. 426-438, (1952).

[2] D. Mugnai, A. Ranfagni, and R. Ruggeri, "Pupils with super-resolution", Phys. Lett. A, v. 311, pp.77-81 (2003);

[3] A. Ranfagni, D. Mugnai, and R. Ruggeri, "Beyond the diffraction limit: Super-resolving pupils", J. Appl. Phys., v. 95, pp. 2217-2222 (2004).

[4] http://www.altairhyperworks.com/product/FEKO

[5] http://www.ifac.cnr.it/PUTO/index.htm

[6] Luca Olmi, Pietro Bolli, Luca Cresci, Daniela Mugnai, Enzo Natale, Renzo Nesti, Dario Panella, and Lorenzo Stefani, "Super-resolution with Toraldo pupils: analysis with electromagnetic numerical simulations", Proc. of SPIE, vol. 9906, pp. 99065Y-1--99065Y-11 (2016). doi: 10.1117/12.2230970.

[7] Luca Olmi, Pietro Bolli, Luca Cresci, Francesco D'Agostino, Massimo Migliozzi, Daniela Mugnai, Enzo Natale, Renzo Nesti, Dario Panella, Lorenzo Stefani, "Laboratory measurements of super-resolving Toraldo pupils for radio astronomical applications", Exp Astron. v. 43, pp. :285–309 (2017) .

[8] Luca Olmi, Pietro Bolli, Luca Carbonaro, Luca Cresci, Daniela Mugnai, Enzo Natale, Renzo Nesti, Dario Panella, Juri Roda and Giampaolo Zacchiroli, "Design of Super-Resolving Toraldo Pupils for Radio Astronomical Applications", Proc. of the 32nd URSI GASS, Montreal (2017)

[9] Luca Olmi, Pietro Bolli, Luca Carbonaro, Luca Cresci, Pasqualino Marongiu, Daniela Mugnai, Enzo Natale, Renzo Nesti, Dario Panella, Juri Roda and Giampaolo Zacchiroli, "Design and Test of a Toraldo Pupil Optical Module for the Medicina Radio Telescope", Proc. of the 2nd URSI AT-RASC, Gran Canaria, 28 May – 1 June 2018 (in press).

[10] L. Olmi, P. Bolli, L. Carbonaro, L. Cresci, A. Maccaferri, G. Maccaferri, P. Marongiu, D. Mugnai, R. Nesti, A. Orfei, D. Panella, S. Righini, "First testa of a Toraldo pupil optical module for the 32m medicina antenna", Proc. of the XXII Riunione Nazionale di Elettromagnetismo, Cagliari, Italy, September 3-8 (2018), in press.

[11] P. A. R. Ade, G. Pisano, C. E. Tucker and S. O. Weaver, "A review of metal mesh filters," Proceedings of SPIE: 6275, 6275U (2006).

[12] G. Pisano, P. Ade, C. Tucker, P. Moseley and M.W. Ng, "Metal mesh based metamaterials for millimetre wave and THz astronomy applications," Proc. 8th UCMMT-2015 Workshop Cardiff, pp.1-4 (2016)

[13] G. Pisano, M.W Ng, B. Maffei and F.Ozturk, "A Dielectrically Embedded Flat Mesh Lens for Millimetre Waves Applications," Applied Optics, v. 52, n.11, pp.2218-2225 (2013),

[14] G. Pisano, M.W. Ng, V. Haynes, B. Maffei, "A Broadband Metal-Mesh Half-Wave Plate for Millimetre Wave Linear Polarisation Rotation", Progress In Electromagnetics Research M, **25**, pp.101-114 (2012).

[15] G. Pisano, B. Maffei, P.A.R. Ade, P. de Bernardis, P. De Maagt, B. Ellison, M. Henry, M.W. Ng, B. Schortt, C. Tucker, "Multi-Octave Metamaterial Reflective Half-Wave Plate for Millimetre and Sub-Millimetre wave Applications," Applied Optics, 55, 10255-10262 (2016).

[16] G. Pisano, P. A. R. Ade, C. Tucker, "Experimental realization of an achromatic magnetic mirror based on metamaterials," Applied Optics, Vol. 55, Issue 18, pp. 4814-4819 (2016)

[17] Ansys HFSS, www.ansys.com

[18] B. Maffei, et al., "Study of corrugated Winston horns," Proc. SPIE, 5498, pp. 812-817 (2004).

Downloaded From: https://www.spiedigitallibrary.org/conference-proceedings-of-spie on 19 Nov 2020
Terms of Use: https://www.spiedigitallibrary.org/terms-of-use